



This article appeared in a journal published by Elsevier. The attached copy is furnished to the author for internal non-commercial research and education use, including for instruction at the authors institution and sharing with colleagues.

Other uses, including reproduction and distribution, or selling or licensing copies, or posting to personal, institutional or third party websites are prohibited.

In most cases authors are permitted to post their version of the article (e.g. in Word or Tex form) to their personal website or institutional repository. Authors requiring further information regarding Elsevier's archiving and manuscript policies are encouraged to visit:

<http://www.elsevier.com/copyright>



Reliable prediction of pore size distribution for nano-sized adsorbents with minimum information requirements

A. Shahsavand*, M. Niknam Shahrak

Chemical Engineering Department, Faculty of Engineering, Ferdowsi University of Mashhad, Mashhad, P.O. Box 91775-1111, Islamic Republic of Iran

ARTICLE INFO

Article history:

Received 25 December 2010
Received in revised form 9 March 2011
Accepted 10 March 2011

Keywords:

Condensation
Adsorption
PSD
Regularization
Cross validation

ABSTRACT

Direct estimation of pore size distribution (PSD) for nano-structured adsorbents suffers from a number of heavy shortcomings. On the other hand, conventional regularization techniques also require profoundly detailed and accurate information about the proper local adsorption isotherm (kernel) to provide reliable PSDs. Selection of improper kernel or use of inexact values for isotherm parameters can lead to serious errors in PSD profiles.

Two new PSD determination techniques are presented in this article for efficient PSD recovery from mere condensation data or condensation isotherms in the presence of adsorption. The second method extends the first approach by considering a pre-adsorbed layer prior to condensation. Both procedures use entirely different linear regularization technique compared to conventional regularization methods. The new proposed techniques do not require any *a priori* information about the shape of local adsorption isotherm. They recruit minimum number of physical data or assumptions to produce reliable performances for successful PSD recoveries.

Several comparative synthetic and real case studies are employed to illustrate the promising performance of the newly proposed Techniques. The leave one out cross validation (LOOCV) criterion and the generalized singular value decomposition (GSVD) technique are crucial for fast, efficient and reliable estimation of optimal regularization level (λ^*). Simultaneous manual verification is also recommended to ensure best possible performance. Although various heuristics are considered for estimation of adsorbed film thickness, however, the proposed method provides almost same result for all different heuristics.

© 2011 Elsevier B.V. All rights reserved.

1. Introduction

Efficient and reliable estimation of pore size distribution (PSD) for heterogeneous solid adsorbents is crucial for successful design and operation of any adsorption process. Direct measurement of PSD is usually expensive and in many practical applications may not be feasible. Multifaceted theories and sophisticated models are required to obtain a realistic estimation of PSD from a set of noisy measured isotherms.

Relatively simple heuristics methods (such as Barret, Joyner and Halenda (BJH), Kruk–Jaroniec–Sayari (KJS), Horvath and Kawazoe (HK) and Nguyen and Do (ND)) were presented from early 1950s to late 1990s by numerous researchers to predict PSD from experimental adsorption isotherms [1–4]. In mid 1980s, Tarazona, Marconi and Evans [5] applied Density Functional Theory (DFT) to the adsorption isotherms. Two types of approximation were employed for the hard-sphere free energy functional.

In 1989, Seaton, Walton and Quirke [6] presented a practical method based on mean-field density functional theory to determine pore size distribution from nitrogen isotherms. However, their approach employed the presumption of a specific distribution function. The proposed method was able to determine both the micropore and mesopore size ranges using a single analysis tool. They used a pre-specified bimodal lognormal distribution and tuned its various parameters to get the measured isotherm. Although they mentioned that the so-called direct method¹ provides infinite number of distributions, however, they claimed that if the local adsorption isotherm consists of 20 or more measured data points, then “two functions that represent the data equally well may have different mathematical forms, their numerical values are very similar”. As it will be clearly illustrated in this article, the infinite number of optimal distributions which satisfies Eq. (1) will be entirely different even for much larger data sets.

In an entirely different approach, the ill-posed problem of finding PSD of a solid adsorbent ($f(r)$) from a set of measured isotherms

* Corresponding author. Tel.: +98 0915 514 9544; fax: +98 511 8816840.
E-mail address: shahsavand@um.ac.ir (A. Shahsavand).

¹ Assuming both distribution ($f(r)$) and kernel ($\theta(P_i, r)$) to reconstruct the measured isotherm from Eq. (1).

data from following integral equation² was achieved using the “inverse theory” [7]. In mathematical terms, the experimental isotherm is the integral of the single pore isotherm multiplied by the pore size distribution. For a slit-shaped pore, this can be written as

$$\Psi(P_i) = \frac{C_{\mu}(P_i)}{C_{\mu \rightarrow s}} = \int_{r_{\min}}^{r_{\max}} \theta(P_i, r) f(r) dr \quad (1)$$

where $\theta(P_i, r)$ is the local adsorption isotherm (kernel) evaluated at bulk pressure P_i and local pore size (r). The function $f(r)$ denotes the PSD of the heterogeneous solid adsorbent. Evidently, a small perturbation in the data $\Psi(P_i)$ will almost certainly result in a substantial alteration in the solution ($f(r)$). In the absence of lateral interactions, the fractional adsorption of an adsorbate on various sites of a solid adsorbent is described by numerous adsorption isotherms such as Linear Driving Force (LDF), Langmuir, Freundlich, Dubinin–Radushkevich (DR), Dubinin–Astakhov (DA), Sips, Toth, Unilan, Jovanovich, Temkin, Brunauer–Emmett–Teller (BET), Fowler and Harkins–Jura. The maximum adsorption capacity $C_{\mu s}$ is only a function of temperature and does not depend on pressure ($C_{\mu s} = C_{\mu s0} \exp[-\beta(T - T_r)]$).

The following literature review emphasises on various researches performed in the latter area which combines inverse theory with linear regularization technique (also known as Phillips–Twomey method or Tikhonov–Miller regularization) to extract pore size distribution from a set of adsorption isotherm data. Two novel techniques will be presented later in this article which both of them enjoy the solid theoretical background of powerful regularization technique to predict PSD from both just condensation data and condensation with a pre adsorbed layer.

In a pioneering work, Merz [8] used the regularization theory and generalized cross-validation (GCV) technique to determine the adsorption energy distribution (AED), using Langmuir and BET isotherm. House et al. [9] used similar approach to predict the energy distribution of a heterogeneous solid adsorbent by employing the second order penalized least square (PLS) technique. They reported that “the obtained results using the regularization method indicate that the solution is entirely dependent on the quality and range of the isotherm data and various approximate solutions may be formulated according to the desired agreement between the computed and experimental isotherms”.

In 1998, Bhatia [10] successfully applied the combination of finite element collocation technique with regularization method to extract various double peak pore size distributions from 100 synthetic isotherm data points contaminated with 1% normally distributed random errors using DR isotherm. They applied the constraint of non-negativity of solutions by simply utilizing a Newton–Raphson technique. Although they reported that “the method is stable over a wide range of values of the regularization parameter”, however, we believe that the application of non-negativity constraint usually provides unrealistic solutions. Therefore, it would be more advantageous to provide non-negative solution without using the above constraint.

Ryu et al. [11] carried out extensive adsorption studies of a series of carbonaceous adsorbents including polyacrylonitrile (PAN)-based activated carbon fibres, coal activated carbon and pitch carbon bead. Nitrogen adsorption measurements were used to evaluate the specific surface area, micropore surface area, micropore volume and PSD. The PSDs of the samples were calculated by employing the regularization method according to Density Functional Theory (DFT) that is based on a molecular model for adsorption of nitrogen in porous solids. Dubinin–Radushkevich

Plots were employed to observe multi stages of adsorption and pore filling procedure. Although the presented method is able to successfully extract the PSD's from several measured isotherms, however, it requires too many parameters (such as: inter-nuclear separation of the molecules, depth of the inter-molecular potential well, molecular diameter, energy and size parameters of carbon–adsorbate interaction, number density of carbon atoms in graphite and the separation of the graphite planes) to achieve this task.

In 1999, Dion and Lasia [12] extracted several AEDs from various synthetic and experimental data sets via regularization technique using Frumkin–Temkin isotherms. They concluded that “the proper choice of regularization parameter is the biggest problem”. This problem can be avoided by resorting to the Leave One Out Cross Validation (LOOCV) criterion [13].

In 2001, Do and Do [14] developed a theory for diffusion and flow of pure sub-critical adsorbates in microporous activated carbon over a wide range of pressure, where capillary condensation is occurring. The complete pore size distribution was required in their theory for the calculation of the Ajax activated carbon permeability. The permeability was found to be dominated by pores having size less than 2 nm or greater than 400 nm. The former is by flow of condensate, while the latter is by Knudsen diffusion and gaseous viscous flow.

Gill et al. [15] used Dubinin–Astakhov isotherm to evaluate the micropore size distribution of several modified carbon molecular sieves. They actually used a nonnegative constraint first order penalized least square cost function but named it as regularization technique. As mentioned earlier, this method was originally used in 1978 by House et al. [9].

In 2005, Herdes et al. [16] computed PSD from experimental adsorption isotherms using regularization procedure. They concluded that “the individual pore model seems to be accurate, provided that an adequate method to generate the kernel of individual adsorption isotherms and a robust mathematical procedure to invert the adsorption integral equation are available”. As it will be pointed out in subsequent sections, selection of inappropriate kernel may lead to misleading pore size distributions.

Segura and Toledo [17] presented the simulation results of pore-level drying of non-hygroscopic liquid-wet rigid porous media for 2D and 3D pore networks. Evaporation and drainage mechanisms were considered under isothermal condition. Details of pore space including pore size distribution and pore shape were used to calculate the effective permeability of liquid and diffusivity of vapor.

In 2006, Solcova et al. [18] provided a large collection of valuable experimental measurements (via mercury porosimetry) for a set of controlled-pore glasses CPG10 with different nominal pore sizes. The measured isotherms and the corresponding PSDs are valuable assets for validation of any new method regarding PSD estimation from condensation or adsorption data sets.

Podkoscielny and Nieszporek [19] used the regularization based INTEG program developed by Jaroniec et al. [20] to predict the non-symmetrical single peak adsorption energy distribution of various activated carbons using a number of experimental adsorption isotherms borrowed from literature [21–23].

Gauden et al. [24] extended the Nguyen and Do method to recover the bimodal PSD of various carbonaceous materials from a variety of synthetic and experimental data. They concluded that “the bimodality of the pore size distribution is a characteristic feature of the majority adsorbents possessing micropores and it results from the similarity of the local adsorption isotherm in the range of the pore widths for which the gap between peaks (related to the primary and secondary micropore filling mechanism) exists”.

In 2008, Kang et al. [25] used chemical vapor deposition method of benzene as a chemical agent to control pore size distribution of activated carbon. Pore size distribution results investigated by

² Known as the Fredholm integral of first kind.

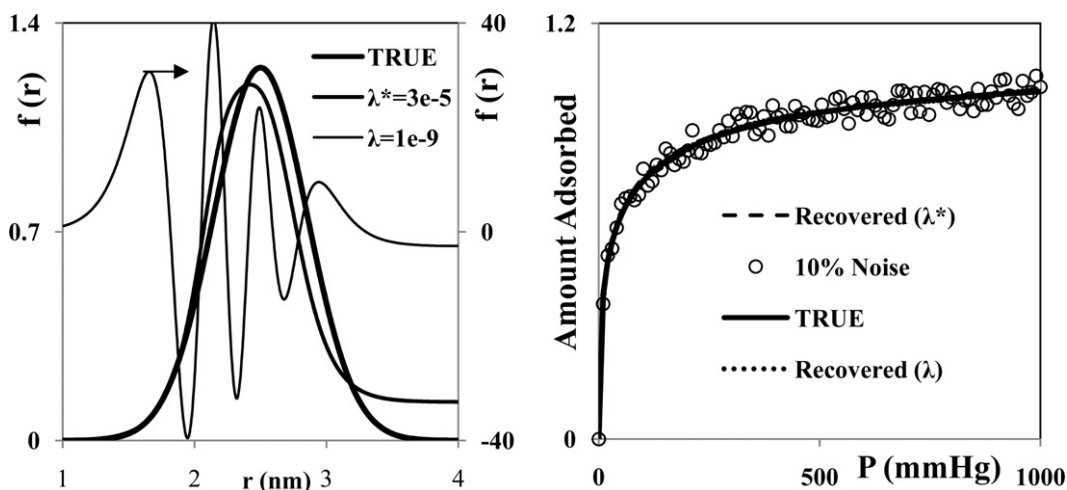


Fig. 1. Unrealistic PSD computed via forward method which exactly recovers the isotherm data.

adsorption of various gases including CO₂ (3.3 Å), n-butane (4.3 Å) and iso-butane (5.0 Å), assured of the pore constriction or heightened energy barrier on the pore opening. They observed that “the nitrogen diffusivity and the selectivity of treated samples are inversely proportioned”. Pore size distribution by BET method also showed that chemical vapor deposition narrowed pores and improved the selectivity of target gas from air.

Choma et al. [26] improved Kruk–Jaroniec–Sayari (KJS) pore size analysis technique to predict the pore size distribution of two different channel-like mesoporous carbons from various sets of Nitrogen and Argon adsorption isotherms. The article does not contain any measured PSD's for validation purposes.

In 2010, Shahsavand and Niknam [27] presented a new regularization based algorithm to extract PSD of heterogeneous solid adsorbents from highly noisy condensation isotherms with almost no *a priori* assumption. The performance of the proposed method was validated using various synthetic and experimental data sets. A brief review of their work is necessary and will be presented in the following section to familiarize the reader with the importance and theoretical background of the newly proposed method.

Development of this new method will be considered in more details. Various correlations will be examined for estimation of the adsorbed film thickness (prior to condensation). Furthermore, a synthetic illustrative example and several real case studies³ will be used to demonstrate the promising performance of the newly proposed method for extraction of PSD from ordinary condensation data when the condensation process preceded by a pre-adsorbed layer. Although, many previous methods accounted for the pre-adsorbed layer during the condensation process in the past few decades, however, to the best of our knowledge, this issue (i.e. extracting PSD via linear regularization theory from condensation isotherm when a pre-adsorbed layer precedes the condensation process) has not been addressed previously.

2. Shortcomings of conventional PSD estimation techniques

As mentioned earlier, various procedures have been used conventionally to extract the pore size distributions of various adsorbents from available adsorption isotherms. In the so called “direct methods”, a pre-specified isotherm was used along with

some assumed distribution (for $f(r)$) and then the corresponding values of $\Psi(P_i)$ were computed by evaluating the integral term of Eq. (1). The proposed distribution was decided to be acceptable, if and only if, the computed isotherm could reconstruct the experimental data [28,29].

It was clearly demonstrated in our recent article [27] that for each local adsorption isotherm (or kernel), infinite distributions (multiple solutions) can theoretically reproduce the adsorption data, while only one of them provide proper distribution for the adsorbent. As shown in Fig. 1, many other sub-optimal solutions (which can successfully filter-out the noise and exactly recover the true underlying isotherm hidden in a set of noisy data) can be entirely inappropriate and may lead to exceedingly misleading distributions.⁴ This is not surprising, because all of these unrealistic distributions are actually the optimal solutions of a minimization problem with no definite physical meaning. Langmuir isotherm has been employed in both synthetic isotherm data generation step and PSD recovery process of Fig. 1.

In the second alternative approach, Eq. (1) can be viewed as the *ill-posed* problem of attempting to extract part of an integrand, $f(r)$, from knowledge of the integral $\Psi(P)$. In principle, this is unsatisfactory as there exists an infinite number of functions $f(r)$ that will be consistent with the measured $\Psi(P)$. Using combination of inverse theory and linear regularization technique, the above ill posed problem can be readily reduced to the solution of the following set of linear equations.

$$(R^T R + \lambda B^T B)f(r) = R^T \underline{\psi} \quad (2)$$

where the elements of the $N \times M$ matrix R are defined by $R_{ij} = \theta(P_i, r_j)(r_{j+1} - r_j)$ and the elements of $(M - 1) \times M$ matrix B depends on the order of regularization technique (used as *a priori* information) [27]. The optimum level of regularization (λ^*) has crucial effect of the recovered PSD and can be efficiently computed by minimizing the LOOCV criterion [13].

$$CV(\lambda) = \frac{1}{N} \sum_{k=1}^N \left[\frac{e_k^T [I_N - H(\lambda)] y}{e_k^T [I_N - H(\lambda)] e_k} \right]^2 \quad (3)$$

$$H(\lambda) = R(R^T R + \lambda B^T B)^{-1} R^T \quad (4)$$

³ For adsorption of nitrogen (in text) and argon (in appendix) on several different adsorbents.

⁴ Note the values of vertical axes on the left and right hand sides of the distribution curves.

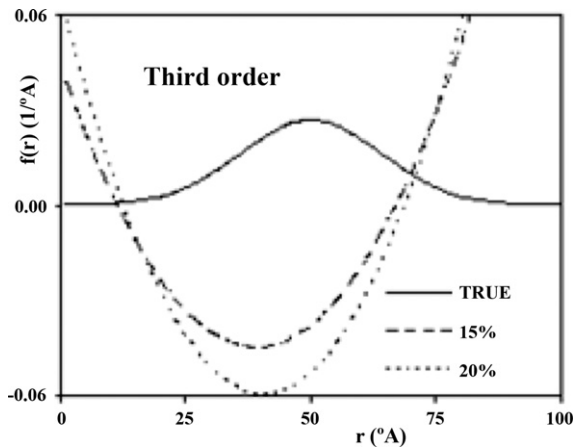


Fig. 2. Dramatic failure of traditional regularization method when dissimilar isotherms are used in data generation step and PSD recovery process.

As mentioned before, numerous kernels $(\theta(P_i, r))$ can be used for a given set of adsorption data and each kernel may lead to entirely a different solution (distribution). Furthermore, in most practical applications, the kernel parameters are almost always estimated by assuming (unconsciously) delta Dirac function for AED or PSD [28,29]. Evidently, such unrealistic parameters are not consistent with the actual pore size or energy distribution. A recursive method should be used to correct the fitted parameters based on the computed distribution.

Fig. 2 illustrates dramatic failure of traditional regularization technique for capturing the PSD of a solid adsorbent from a set of synthetic noisy isotherm. Different local adsorption isotherms were employed in the isotherm generation and PSD extraction stages. Langmuir isotherm was used in the process of synthetic data generation. Afterwards, the contaminated data (with 1% and 20% noise levels) sets was recruited to predict PSD of the adsorbent by replacing Langmuir with Sips local adsorption isotherm. We would like to emphasize that the traditional regularization technique can easily lead to severely unrealistic distributions, if inappropriate choice of kernel is selected. Both newly proposed methods do not require any knowledge about kernel and provide reliable PSDs with minimum required information.

3. Mathematical issues

The above synthetic example clearly showed that appropriate choice of kernel is essential for successful recovery of PSD via traditional regularization technique. Therefore, it would be extremely advantageous if the kernel term in Eq. (1) can be omitted. Fortunately, in the absence of appreciable adsorption and for the case of mere condensation of a substance on pores of a solid (smaller than the threshold radius r_K), the following equation can be used instead of Eq. (1).

$$\Psi(P_i) = \int_0^{r_K(P_i)} f(r) dr \quad (5)$$

The threshold radius for both condensation and evaporation cases can be computed from the Kelvin equation [27]. For solids exhibiting an adsorbed layer with specific thickness (t) prior to condensation, the total amount of adsorbed material at a given pressure

(P_i) for cylindrical pores⁵ can be computed via [4,29]⁶:

$$\Psi(P_i) = \int_0^{r_K(P_i)} f(r) dr + t \int_{r_K(P_i)}^{r_{max}} \frac{2f(r)}{r} dr \quad (6)$$

where $f(r)$ is the pore size distribution of the solid adsorbent and $r_K(P_i)$ is the corrected pore radius calculated from Kelvin equation at the corresponding adsorption pressure ($r_K = r_K + t$). The statistical adsorbed film thickness (t) can be calculated as a function of pressure from a variety of available correlations. This issue will receive more attention in the next sections,

As it was fully discussed in our previous article [27], the following section briefly explains how to recover PSD from pure condensation data. A more robust and new technique will be presented in Section 3.2 which is able to extract PSD from both only condensation isotherms and for the cases where the condensation process is accompanied with a single adsorption layer (Eq. (6)).

3.1. Mere condensation condition

The required PSD from pure condensation data can be computed using the following partitioned matrix derived from Eq. (5) [27]:

$$(R^T R) f_{\lambda} = R^T \Psi \quad (7)$$

where $N \times M_t$ matrix $R \in \Re^{[N \times \sum_{i=1}^N M(P_i)]}$ has usually many more columns than its rows, the overall PSD column vector $(f_{\lambda} \in \Re^{[\sum_{i=1}^N M(P_i) \times 1]})$ has dimensions of $[\sum_{i=1}^N M(P_i) \times 1]$ and Ψ is a $[N \times 1]$ vector. Matrix R is a lower triangular partitioned matrix as described in [27].

Almost always, the $M_t \times M_t$ matrix $R^T R$ is ill-conditioned or nearly singular. Hence, direct estimation of PSD from Eq. (7) is hopeless and leads to extremely oscillatory solution. Using the proper order of regularizations [7,27], the above equation can be rewritten as:

$$(R^T R + \lambda B^T B) f_{\lambda} = R^T \Psi \quad (8)$$

The required pore size distribution may then be calculated by resorting to GSVD technique coupled with minimization of CV criterion [13]. Fig. 10SI⁷ illustrates the remarkable performance of our previously proposed method (SHN1⁸) for successful extraction of required PSD's from various real experimental condensation isotherms borrowed from literature [18,27]. Note that the proposed method always performs better from all other techniques used recently in 2006 by Solocova et al. [18] and provides excellent match with mercury porosimetry data.

3.2. Condensation with prior adsorption

Although the newly proposed method performs brilliantly on extraction of PSD from condensation data, however, it may not provide optimal distributions when the adsorption process becomes more and more important. Fig. 3 compares typical performance of our previous method (SHN1) and other available techniques with the newly proposed method (SHN2⁹) for recovery of PSD from two different condensation isotherms. The first set belongs to mere

⁵ For slit shape pores, the multiplier (2) in the second right hand term vanishes [35].

⁶ It is recommended to see our previous article [27] for elementary discussion on adsorption modeling.

⁷ Online supporting information.

⁸ Stands for Shahsavand–Niknam previous (first) method [27].

⁹ Stands for Shahsavand–Niknam present (second) method .

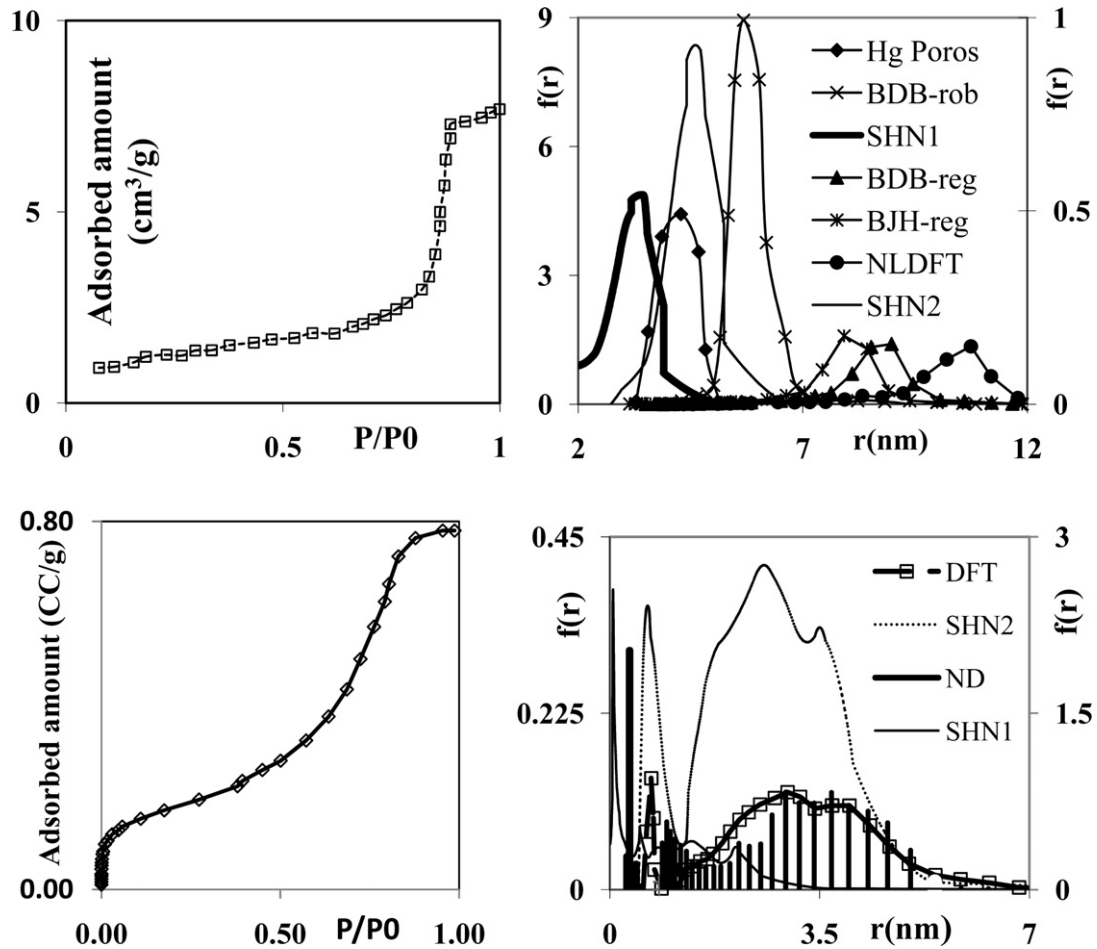


Fig. 3. Comparison of our two proposed method (SHN1 and SHN2) with other techniques applied recently (2006) [18] for PSD recovery from mere condensation isotherm (CPG 75) and condensation accompanied with prior adsorption (Carbosilab-1) [18,30].

condensation process while the second set comes from condensation with a prior adsorption layer. Both of our methods (SHN1 and SHN2) perform very adequately for mere condensation processes. As it can be seen, our previous method (SHN1) relatively fails when the condensation is accompanied with a pre-adsorbed layer. While, the new proposed method (SHN2) performs very adequately and provides impressive performances on PSD recovery of meso-porous and micro-porous materials. The mercury porosimetry data for PSD shown in Fig. 3 was borrowed from literature [18]. Both new methods perform better than the traditional techniques (e.g. BDB-rob, BDB-reg, BJH-reg¹⁰ and NLDFT¹¹ which were used very recently only a few years ago [18]) on pinpointing the peak location from mere condensation isotherm but it is much simpler to use for practical applications and requires far less physical data or a priori assumptions.

As mentioned earlier, for solids exhibiting an adsorbed layer with specific thickness (t) prior to condensation, the total amount of adsorbed material at a given pressure (P_i) for cylindrical pores¹² of radius r , can be represented by Eq. (6). The statistical adsorbed film thickness (t) can be calculated as a function of total adsorbed amount (Ψ), monolayer adsorbed amount (Ψ_m) and monolayer

adsorbed film thickness (t_m) from the following equation [29,31]:

$$t(\text{nm}) = t_m(\text{nm}) \left[\frac{\Psi}{\Psi_m} \right] \quad (9)$$

The value of t_m depends on the method of stacking successive layers. For nitrogen, if cubical packing is assumed, $t_m = \sqrt{16.2} = 4.02 \text{ \AA}$ (0.402 nm) while a more open packing will give a value of 0.43 nm. For hexagonal close packing of any adsorbate gas the monolayer adsorbed film thickness should be calculated via [31]:

$$t_m = \frac{MV_S}{Na} \quad (10)$$

where M is the gas molecular weight, V_S is the liquid specific volume at saturation temperature, N is the Avogadro constant and a is the area occupied by one molecule. For nitrogen adsorption at 77 K the monolayer adsorbed film thickness is computed as follows [29]: $t_m = \frac{28 (\text{kg/kg mol}) \times 0.001237 (\text{m}^3/\text{kg})}{6.023 \times 10^{23} (\text{molecule/g mol}) \times 16.2 \times 10^{-20} (\text{m}^2/\text{molecule})} = 0.354 \text{ nm}$ Furthermore, the adsorbed film thickness may also be obtained in terms of p (relative pressure $p = P/P_0$) by combining the BET equation with Eq. (9) to give [4,32]:

$$t = \frac{Ct_m p}{(1-p)[1+(C-1)p]} \quad (11)$$

where the coefficient C is a measure of the adsorptive power on a unit surface is defined as follows: $C = A e^{(\varepsilon_A - \varepsilon_1)}$; $\varepsilon_A = \frac{Q}{RT}$ and $\varepsilon_1 = \frac{\lambda}{RT}$. The exponent factor A is the characteristic of the solid material, parameter Q is the energy of interaction between the first layer of adsorbate and the surface and λ is the heat of liquefaction. Same as BET equation, Eq. (11) usually over predicts the

¹⁰ In Fig. 4 (top right), reg stands for the regularization technique.

¹¹ Broekhoff-de Boer, Barret, Joyner and Halenda and Nonlocal density functional theory.

¹² For slit shape pores, the multiplier (2) in the second right hand term vanishes when the pore radius (r) is replaced by pore width (x) [30].

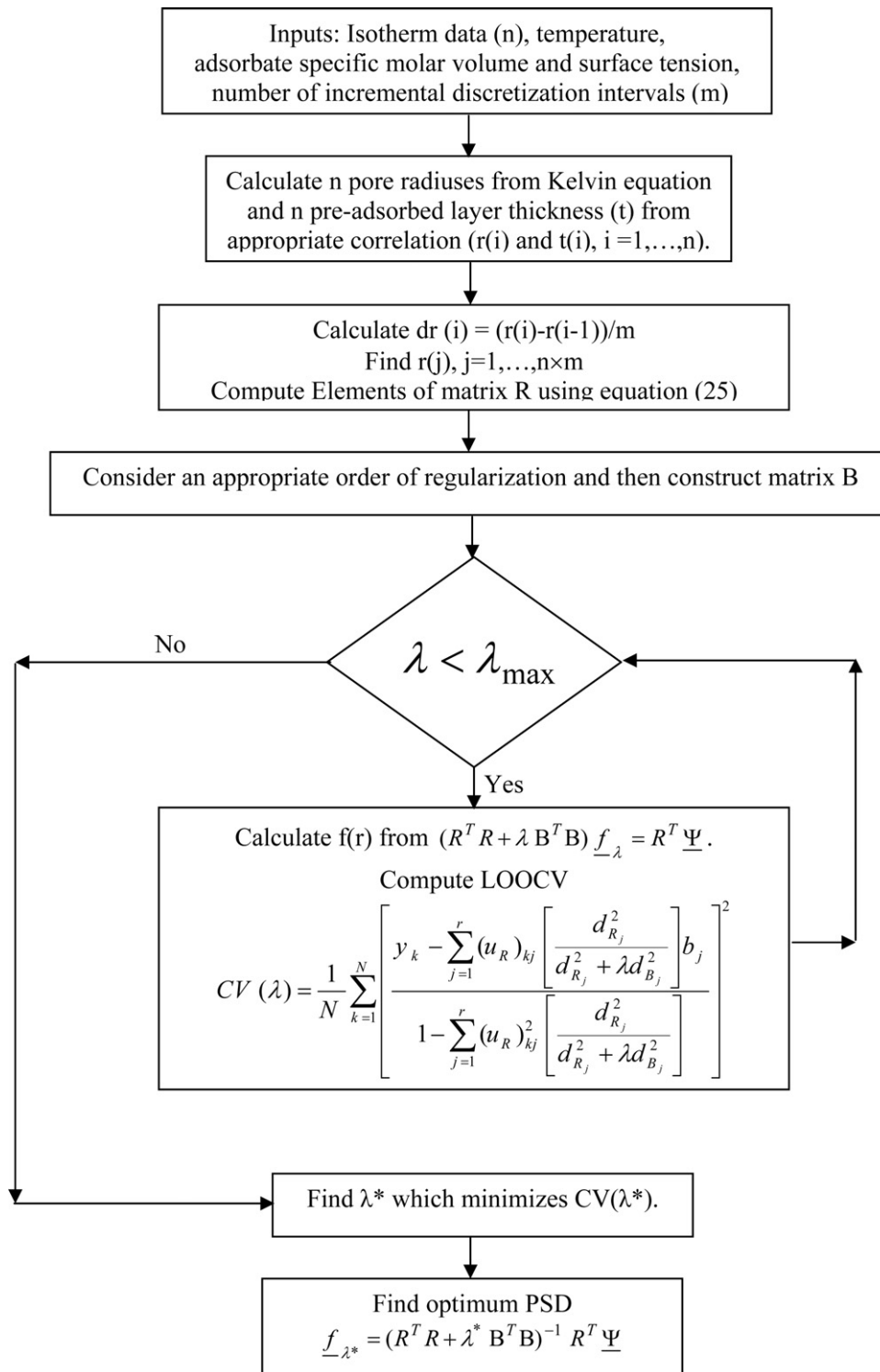


Fig. 4. Flow chart for the calculation procedure of the newly proposed method (SHN2).

value of t in high pressure region. Several correlations have been presented in the literature for computation of adsorbed film thickness from relative pressure. Halsey, Franklin–Halsey–Hill (FHH), Harkins and Jura (Haju), Deboer (Db), Micromeritics¹³ (Micro), Broekhoff and deBoer (BdB) and Nguyen and Do (ND) proposed

the following equations, respectively [4,30,31,33]:

$$t(\text{nm}) = t_m(\text{nm}) \left[\frac{5}{\ln(P_0/P_i)} \right]^{1/3} \tag{12}$$

$$t(\text{nm}) = t_m(\text{nm}) \left[\frac{2.75}{\log(P_0/P_i)} \right]^{1/2.99} \tag{13}$$

$$t(\text{nm}) = \left[\frac{0.1399}{0.034 - \log(P_i/P_0)} \right]^{1/2} \tag{14}$$

¹³ Presented by Micromeritics company.

$$\log\left(\frac{P_i}{P_0}\right) - 0.1682e^{-1.137t(\text{nm})} + \frac{0.1611}{t(\text{nm})^2} = 0 \quad (15)$$

$$t(\text{nm}) = \frac{0.559}{(\log(P_0/P_i))^{0.399}} \quad (16)$$

$$\begin{cases} \log(P_0/P_i) - \frac{0.1399}{t_e(\text{nm})^2} + 0.034 = \frac{2.02^5}{10(r(\text{nm}) - t_e(\text{nm}))} & t_e < 1 \text{ nm} \\ \log(P_0/P_i) - \frac{0.1611}{t_e(\text{nm})^2} + 0.1682e^{-1.137t_e(\text{nm})} = \frac{2.02^5}{10(r(\text{nm}) - t_e(\text{nm}))} & t_e > 1 \text{ nm} \end{cases} \quad (17)$$

$$t(\text{nm}) = t_m(\text{nm}) \left[\frac{Cp}{1-p} \right] \left[\frac{1 + (nf/2 - n/2)p^{n-1} + (nf+1)p^n + (nf/2 + n/2)p^{n+1}}{1 + (C-1)p + (Cf/2 - C/2)p^n - (Cf/2 + C/2)p^{n+1}} \right] \quad (18)$$

where n is the number of adsorbate layers ($n = r/t_m$), $f = e^{\Delta\varepsilon_1}$, $t = t_e(1 - t_e/2r)$ and $\Delta\varepsilon_1$ is the excess of the reduced evaporation heat due to interference of the layering on the opposite wall. As it can be seen, the adsorbed film thicknesses in the two latter equations are function of both relative pressure and pore radius. Furthermore, Eq. (17) is derived for adsorption of nitrogen at 78 K and should not be used for other adsorbates. Kruk and Jaroniec also proposed the following empirical correlation for prediction of the nitrogen statistical film thickness on the MCM-41 surface in the relative pressure range of 0.1–0.95 [34]:

$$t(\text{nm}) = 0.1 \left[\frac{60.65}{0.03071 - \ln(P_i/P_0)} \right]^{0.3968} \quad (19)$$

Fig. 20SI compares various plots of nitrogen pre-adsorbed film thickness (t) for Eqs. (12)–(19) (the average pore size is considered 2.5 nm for use in Eqs. (17) and (18)).

With any of the above calculated film thicknesses, the improved threshold radius r_k corresponding to a gas phase of pressure P_i can be computed for adsorption and desorption processes respectively via [29]:

$$r_k(P_i) = t(P_i) + \frac{v_M\sigma}{RT \ln(P_0/P_i)} \quad (20)$$

$$r_k(P_i) = t(P_i) + \frac{2v_M\sigma \cos\theta}{RT \ln(P_0/P_i)} \quad (21)$$

The following section uses Eq. (6) to provide a relatively simple procedure for estimation of pore size distribution from condensation data when accompanied with a pre-adsorbed layer.

3.2.1. Theoretical aspects

For the case of mere condensation, the required pore size distribution was traditionally found by differentiating the first right hand side term of Eq. (6) and using the Kelvin equation (second right hand side term of Eq. (20)) to plot $\Delta\Psi(P_i)/\Delta r(P_i)$ versus $r(P_i)$. In almost all practical situations, the condensation is usually preceded by a pre-adsorbed layer and the traditional approach can lead to severe error by neglecting this pre-adsorbed layer.

As our first trial, the same approach was extended by differentiation Eq. (6) with respect to pore size which leads to following equation:

$$\frac{d\Psi(P_i)}{dr(P_i)} = f_1(r) + \frac{2t(P_i)f_2(r)}{r(P_i)} + \frac{2dt(P_i)}{dr(P_i)} \int_{r_k(P_i)}^{r_{\max}} \frac{f_2(r)}{r} dr \quad (22)$$

where $f_1(r)$ is the pore size distribution for the range of $0 \leq r \leq r_k(P_i)$ and $f_2(r)$ is the pore size distribution for the range of $r_k(P_i) \leq r \leq r_{\max}$. Evidently, the actual pore size distribution of the solid adsorbent will be simply the summation of $f_1(r)$ and $f_2(r)$. The following relatively difficult, time consuming and inexact procedure may be used to compute the required PSD from Eq. (22):

- Assume a distribution for $f_2(r)$ and compute $\int_{r_k(P_i)}^{r_{\max}} f_2(r)/r dr$.
- Calculate $t(P_i)/dr(P_i)$ using one of Eqs. (12)–(19) along with Kelvin equation.
- Compute $\xi(P_i) = 2dt(P_i)/dr(P_i) \int_{r_k(P_i)}^{r_{\max}} f_2(r)/r dr$.
- Assuming $f_1(r) = \Delta\Psi(P_i)/\Delta r(P_i)$ from traditional approach, then $f_2(r)$ can be found by plotting $-r(P_i)\xi(P_i)/2t(P_i)$ versus $r(P_i)$ (using Kelvin equation for $r(P_i)$ along with appropriate correlation for $t(P_i)$).
- Return to step (a) if $f_2(r)$ is not converged.
- Find actual distribution by mere summation of $f_1(r)$ and $f_2(r)$.

In an alternative approach which is much simpler and requires no a priori information about the shape of pore size distribution and provides more exact solution, Eq. (6) can be replaced by the following “quadrature like” summation for N isotherm data, other than origin (0,0):

$$\begin{aligned} \Psi\left(\frac{P}{P_0}\right) &= \sum_{k=1}^i M(P_k) f(r_j) \times \left(\frac{r_{j+1} - r_{j-1}}{2}\right) \\ &+ t \sum_{i=1}^N M(P_i) \frac{2f(r_i)}{r_i} \times \left(\frac{r_{i+1} - r_{i-1}}{2}\right); \quad i = 1, 2, \dots, N \end{aligned} \quad (23)$$

where r_j varies between zero and $r_k(P_i)$ and r_l adapts a value between $r_k(P_i)$ and $r_{k,\max}$. Also $M(P_k)$ is the number of discretized intervals between $r_k(P_{i-1})$ and $r_k(P_i)$. The total number of discretization points is then equal to: $M_t = \sum_{i=1}^N M(P_i)$. Once again, we are not usually interested in every point of the continuous function $f(r)$ and a large number M_t of (preferably) evenly spaced discrete points $r_{k,j}$, $j = 1, 2, \dots, M_t$ will suffice. Analogous to our previous work, the above equation can be easily represented by the following partitioned matrix:

$$R \cdot \underline{f} = \underline{\Psi} \quad (24)$$

where $N \times M_t$ coefficient matrix $R \in \Re \left[N \times \sum_{i=1}^N M(P_i) \right]$ has usually many more columns than its rows, the overall PSD column vector ($f \in \Re \left[\sum_{i=1}^N M(P_i) \times 1 \right]$) has dimensions of $\left[\sum_{i=1}^N M(P_i) \times 1 \right]$ and Ψ is an $[N \times 1]$ vector. Eq. (24) can be expanded as:

$$\begin{bmatrix} \Delta r_1 & \frac{2t_1}{r_{P_2}} \times \Delta r_2 & \dots & \frac{2t_1}{r_{P_N}} \times \Delta r_N \\ \Delta r_1 & \Delta r_2 & \dots & \frac{2t_2}{r_{P_N}} \times \Delta r_N \\ \cdot & \cdot & \cdot & \cdot \\ \cdot & \cdot & \cdot & \frac{2t_N}{r_{P_N}} \times \Delta r_N \\ \Delta r_1 & \Delta r_2 & \dots & \Delta r_N \end{bmatrix} \begin{bmatrix} f_1(r) \\ f_2(r) \\ \cdot \\ \cdot \\ f_N(r) \end{bmatrix} = \begin{bmatrix} \Psi_1 \\ \Psi_2 \\ \cdot \\ \cdot \\ \Psi_N \end{bmatrix} \quad (25)$$

where $[\Delta r_i, i = 1, \dots, N]$ is a row vector with elements equals to the selected increment lengths between two adjacent pressures $[\Delta r_i = (r_k(P_i) - r_k(P_{i-1})) / M(P_i)]$ and $f_i(r)$ is a column vector representing the PSD between $r_k(P_{i-1})$ and $r_k(P_i)$. The ultimate PSD is then again the summation of all individual distributions $[f_i(r), i = 1, \dots, N]$. Since matrix R has much greater number of columns than its rows, therefore, the minimum norm concept

Table 1
Equations of various true pore size distributions considered for synthetic example.

Distribution	Function
Single peak Gaussian	$f(r) = 0.9 \exp(-[(r-12)/4]^2)$
Double peak Gaussian	$f(r) = \exp(-[(r-7)/2]^2) + 0.8 \exp(-[(r-15)/1.5]^2)$
Triple peak Gaussian	$f(r) = \exp(-[(r-3)^2]) + 0.7 \exp(-[(r-10)/1.5]^2) + 0.9 \exp(-[(r-18)/2]^2)$
Ramp function (piecewise linear function)	$\begin{cases} f(r) = 0.1r - 0.5 & 5 \leq r \leq 12 \\ f(r) = -0.1r + 1.9 & 12 \leq r \leq 19 \end{cases}$ Otherwise : $f(r) = 0$

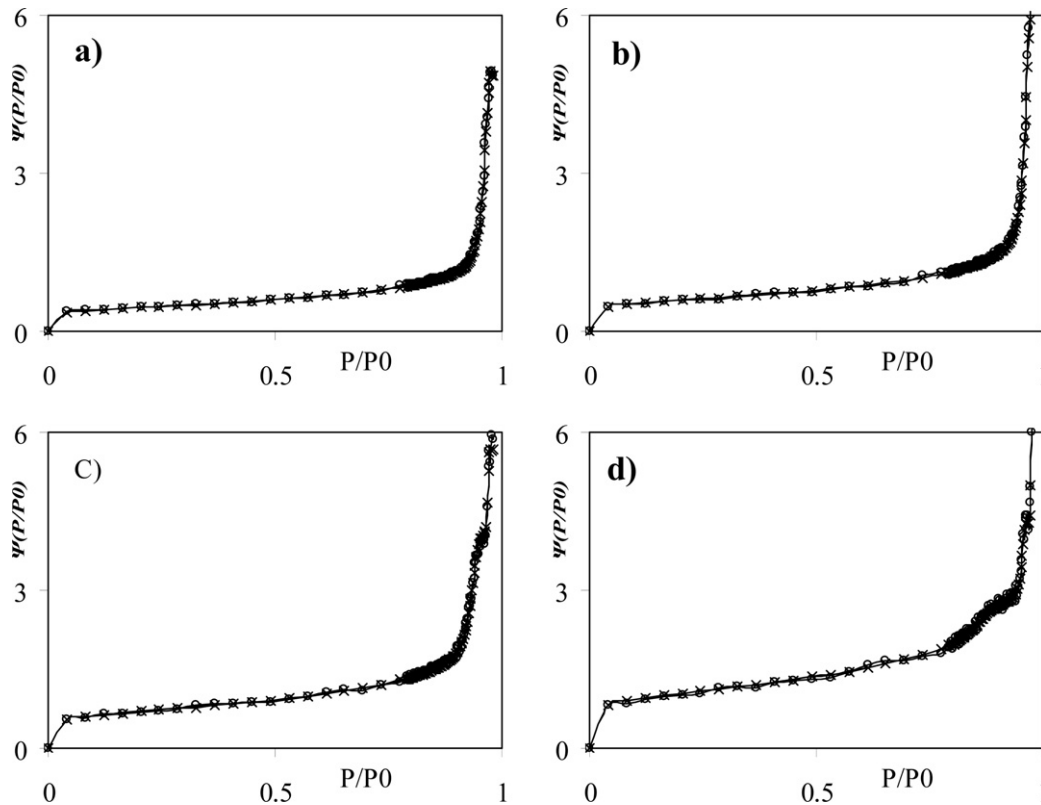


Fig. 5. Actual and noisy (1%: × and 5%: (o)) synthetic isotherms. (a) Double sided ramp. (b) Single Gaussian. (c) Double peak Gaussian. (d) Triple peak Gaussian.

$(\|Rf - \underline{\Psi}\|^2)$ should be used again to compute the required PSD from the solution of following set of linear equations:

$$(R^T R)_{\lambda} f_{\lambda} = R^T \underline{\Psi} \quad (26)$$

In almost all practical applications, the $M_t \times M_t$ matrix $R^T R$ is ill-conditioned or nearly singular due to noisy data. Hence, direct estimation of PSD from Eq. (26) is again hopeless and leads to extremely unrealistic oscillatory solution. As in our previous work [27], the above equation can be rewritten as following by resorting to regularizations technique:

$$(R^T R + \lambda B^T B)_{\lambda} f_{\lambda} = R^T \underline{\Psi} \quad (27)$$

The required pore size distribution may then be calculated by resorting to generalized singular value decomposition (GSVD) technique coupled with minimization of leave one out cross validation (LOOCV) criterion. Fig. 4 presents a typical flow chart for the above calculation procedure. The following synthetic examples demonstrate the effectiveness of the new proposed approach.

4. An illustrative synthetic example

Using similar procedures as our previous article, various noisy data sets each containing of 100 non-equispaced data points were generated employing different PSDs of Table 1 in

the range of $[0 < r < 25 \text{ nm}]$. Both data sets were divided into two separate clusters for isotherm calculations. The primary cluster contained 20 percent of data points in the domain of $[0 < P_i/P_0 < 0.8]$ and the other cluster consisted of the remaining 80% data points in the domain of $[0.8 < P_i/P_0 < 1]$. Eq. (6) was used to generate synthetic isotherms for nitrogen using Halsey equation¹⁴ for adsorbed film thickness and the data are then contaminated with pre-specified (1% and 5%) noise levels. Fig. 5 compares the computed noisy isotherms with truth for different PSDs.

Fig. 3OSI demonstrates the optimal performances of new proposed technique (SHN2) for recovery of a pre-specified true ramp function PSD from various noisy data sets using different orders of regularizations. Figs. 4OSI–6OSI illustrate similar performances for single, double and triple peak Gaussians (Table 1) as true pore size distributions. All predictions were computed using the optimum levels of regularization (λ^*) which were found via LOOCV method and verified manually. Table 2 presents the optimum values of regularization parameter for each case.

As it can be seen in Figs. 3OSI–6OSI, the new proposed method (SHN2) provides excellent prediction for pore size distributions

¹⁴ For nitrogen: $t(\text{nm}) = 0.354[5/\ln(P_0/P_i)]^{1/3}$.

Table 2
Optimum levels of regularization (λ^*) for various true PSDs and different noise levels using several orders of regularization.

Distribution	1% noise				5% noise			
	Zero	First	Second	Third	Zero	First	Second	Third
Single peak Gaussian	0.01024	5.2	671	1.72×10^5	0.06029	20.9	10,737	1.37×10^6
Double peak Gaussian	0.00706	0.222	107	1599	0.0168	3.872	1105	94,806
Triple peak Gaussian	0.001	0.3452	40.5	4830	0.002	2.5547	186	1.98×10^5
Ramp function	0.01051	1.44	44.58	1067	0.044	11.74	4325	8.17×10^5

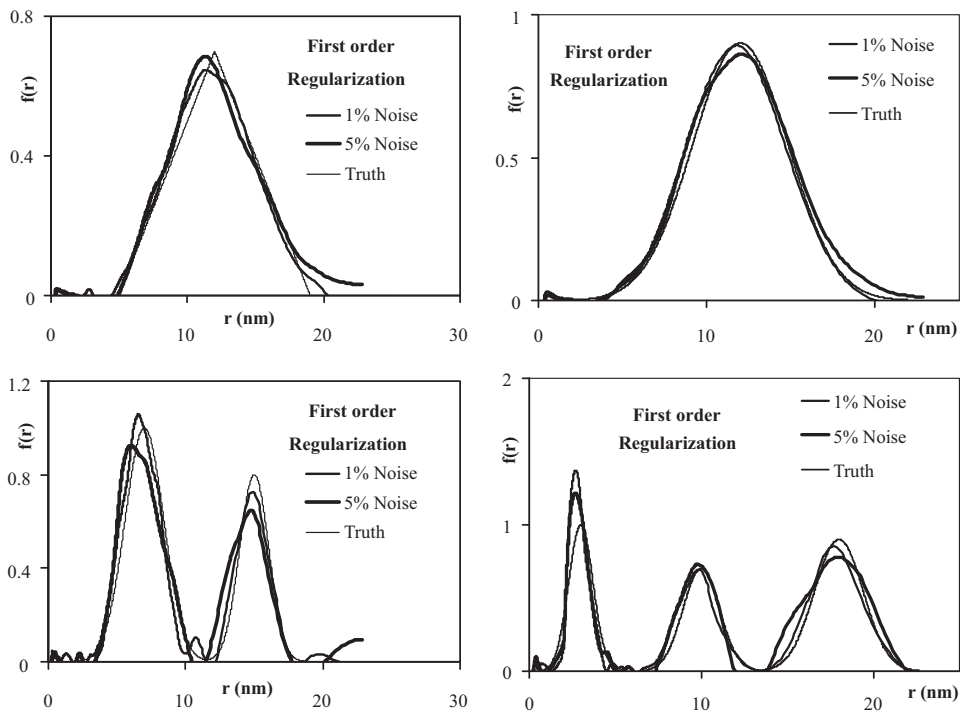


Fig. 6. Optimal PSD recovery performance (λ^*) of the new proposed method for recovery of true ramp function, single, double and triple Gaussian peaks distribution from different noisy data sets using first order regularization technique.

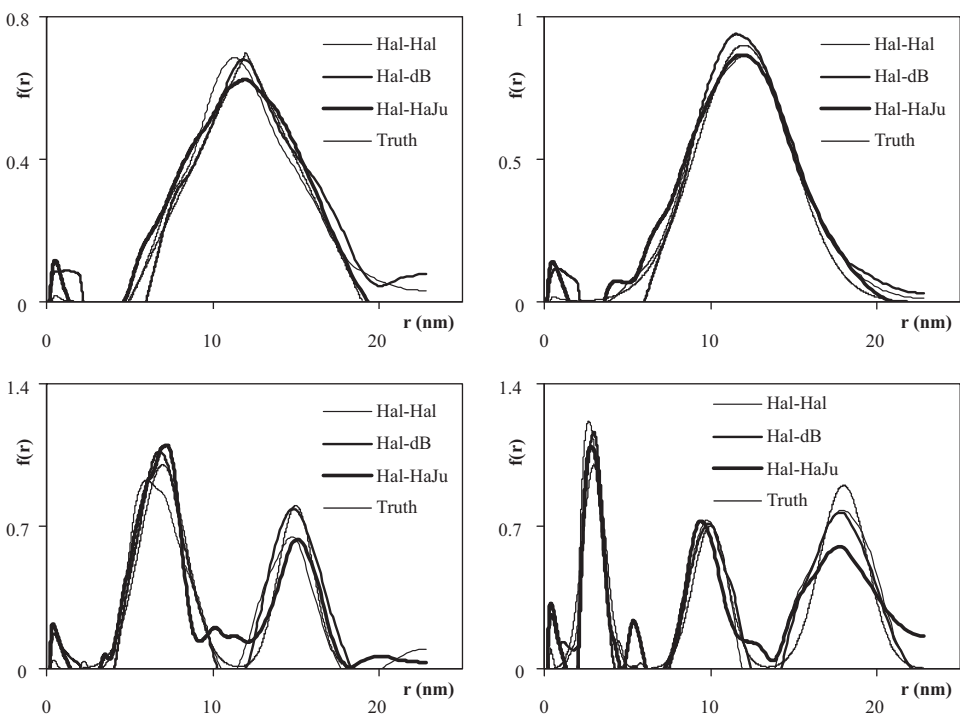


Fig. 7. Optimal PSD recovery performance of the new method using Halsey relation in generation step and Haju & dB correlations in recovery (5% noise, first order regularization).

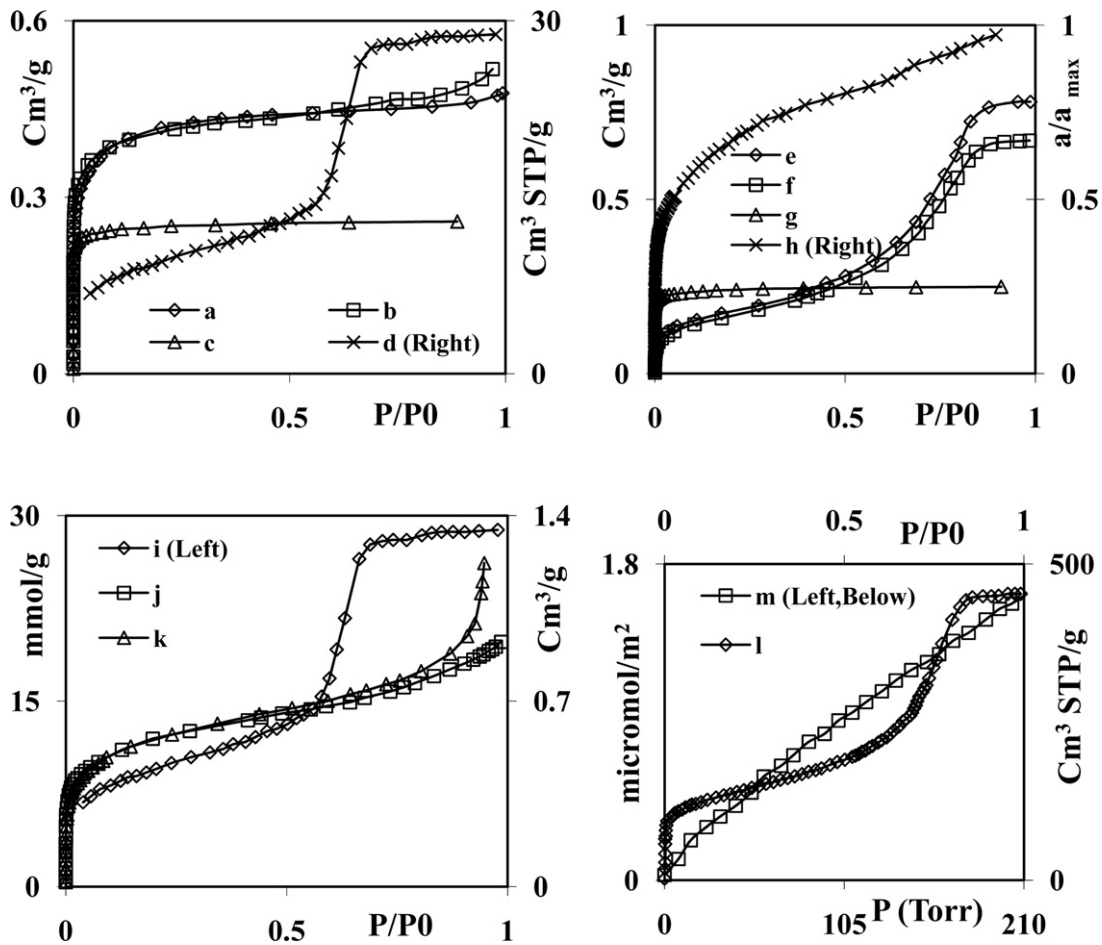


Fig. 8. Various isotherms borrowed from literature (N₂: 77 K, C₆H₆: 373 K). Adsorption of Nitrogen on (a) D43/1 [30], (b) F 300 [30], (c) C873Cu [30], (d) Si-100 [35], (e) carbosil ab-1 [30], (f) carbosil ab-4 [30], (g) C873 [30], (h) PICA HP [36], (i) MCM-41 [37], (j) PAN ACF 2 [30], (k) PAN ACF 3 [30], (l) CMC-1 [26], and finally (m) adsorption of benzene on Si-100 [35]

when appropriate order of regularization with optimum regularization level have been employed. Fig. 6 illustrates the selected performances of our newly proposed method for various PSDs using first order regularization technique at optimum levels of regularization.

In all above predictions, the Halsey correlation was used for prediction of adsorbed film thickness in both isotherm generation step and PSD recovery. Figs. 7 and 7OSI compare the typical optimally recovered PSDs (via the new proposed method) when other correlations were used for calculation of the adsorbed film thickness in PSD recovery steps. In all cases, Halsey correlation was used in generation steps while Harkins and Jura (Hal-HaJu), Deboer (Hal-dB), Micromeritics (Hal-Micr), and Kruk and Jaroniec (Hal-KJ) correlations were employed respectively in the PSD recovery operations. Evidently, the new proposed method performs adequately for all choices of adsorbed film thickness correlations. In other words, the choice of correlation used for estimation of adsorbed film thickness is not crucial.

Table 3
The only physical data required for PSD recovery with the new proposed method [27].

Description	Symbol	Unit	Value	Remarks
Adsorbate (N ₂) surface tension	σ	N/m	8.72×10^{-3}	At 77 K
Adsorbate liquid molar volume	v_M	m ³ /g mol	3.468×10^{-5}	-
Contact angle	θ	rad	0	-

5. Real case studies

In the previous section, the impressive performance of our new proposed method (SHN2) was illustrated using various noisy data sets and different correlations for calculation of pre-adsorbed film thickness. In this section, the capabilities of the new method (SHN2) will be put in to test by using various real data (isotherms) borrowed from literature.

Fig. 8 shows various measured isotherms for adsorption of nitrogen on different adsorbents [30,35–37]. These real isotherms are used to compare the performances of several available techniques (including ours) for PSD recovery. The initial loadings in all isotherms clearly indicate the existence of a pre-adsorbed layer prior to the condensation process or mere adsorption on the solid adsorbent. Table 3 provides all the required physical properties of nitrogen for PSD recovery via the new method (SHN2).

Figs. 9, 8OSI and 9OSI compare various PSD recovery performances of our new method (SHN2) with traditional PSD estimation

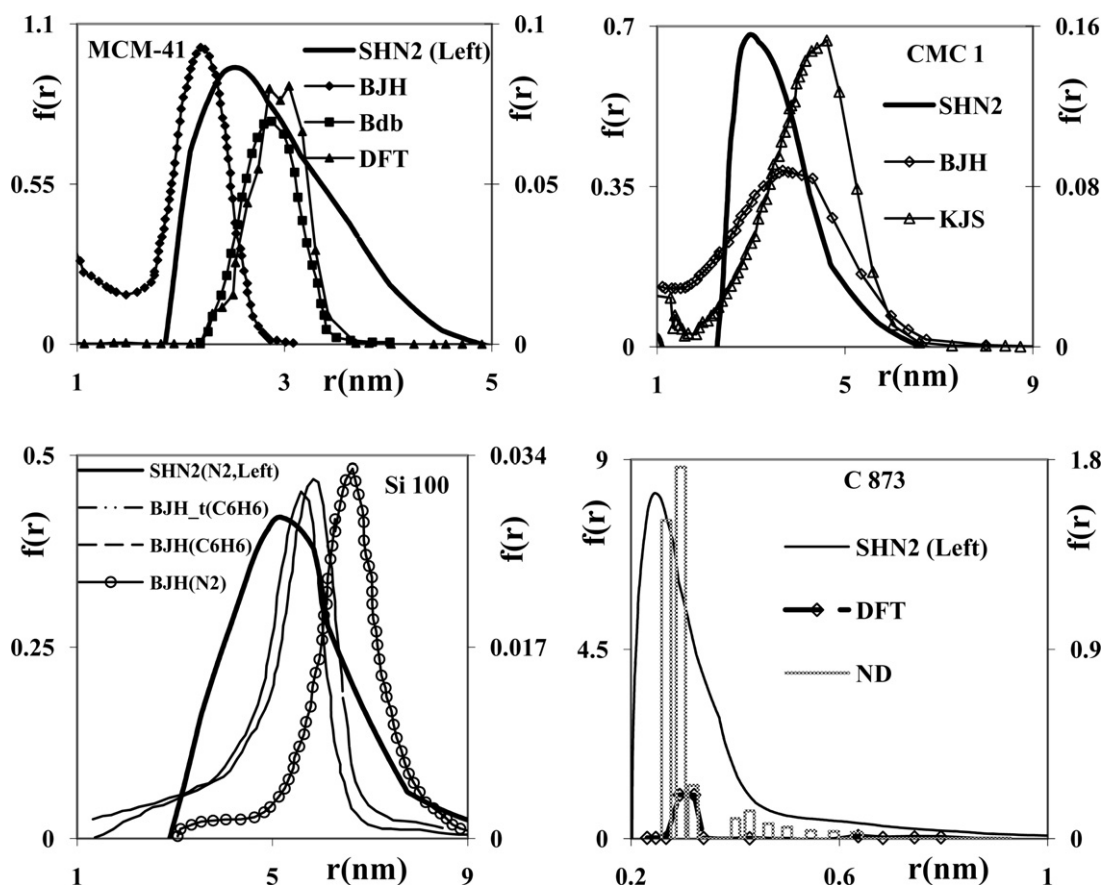


Fig. 9. Comparison of the new method performance with BJH, Bdb, KJS, DFT and ND techniques for single peak PSD recovery of various adsorbents from nitrogen and benzene adsorption isotherm [26,30,35,37].

techniques, using the condensation and adsorption data sets presented in Fig. 8. Several other real case studies are also presented in Figs. 10–13 of Online supporting information (10OSI–13OSI). Evidently, the new technique performs very adequately for almost all real case studies including single peak and multiple peak pore size distributions.

Fig. 10 compares the typical performance of the new method (SHN2) when different correlations are used calculation of for pre-adsorbed film thickness (t) in the PSD recovery process of MCM41. Once again, the new method performs very adequately for almost

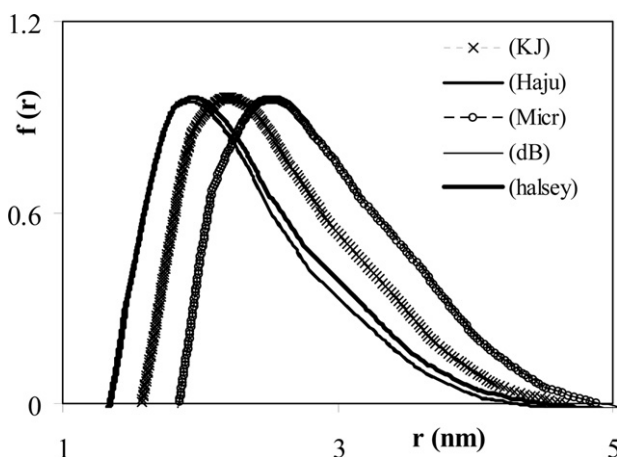


Fig. 10. Comparison of the new method performance for PSD recovery of MCM41 adsorbent using various correlations for calculation of pre-adsorbed layer film thickness (t).

all cases and its impressive performance has not been affected by the choice of pre-adsorbed film thickness calculation procedure. The recovered PSDs for three correlations of dB, Halsey and HaJu (for computing t) are practically the same and it is almost impossible to distinguish between them.

6. Conclusion

A new method was presented in this article for reliable estimation of pore size distribution of heterogeneous solid adsorbents using simultaneous condensation and adsorption isotherms. The proposed method is an extension of our previous method described in full details elsewhere [27].

Numerous experimental data were used from literature to compare the impressive performance of the new method with traditional techniques available for pore size distribution estimation. The new method (SHN2) is simple, versatile and requires minimum number of assumptions or *a priori* information while enjoying a relatively solid theoretical background. It also employs powerful mathematical toolboxes such as linear regularization theory and leave one out cross validation criterion for optimal stabilization of the recovery process. It was clearly shown that the proposed technique provided adequate PSD recovery performances for mere condensation processes or in various conditions where a pre-adsorbed layer precedes the condensation.

Appendix A. Supplementary data

Supplementary data associated with this article can be found, in the online version, at doi:10.1016/j.cej.2011.03.049.

References

- [1] E.P. Barrett, L.G. Joyner, P.P. Halenda, The determination of pore volume and area distributions in porous substances. I. Computation from nitrogen isotherms, *J. Am. Chem. Soc.* 73 (1951) 373–380.
- [2] M. Kruk, M. Jaroniec, A. Sayari, Application of large pore MCM-41 molecular sieves to improve pore size analysis using nitrogen adsorption measurements, *Langmuir* 13 (1997) 6267–6273.
- [3] G. Horvath, K. Kawazoe, Method for the calculation of effective pore size distribution in molecular sieve carbon, *J. Chem. Eng. Jpn.* 16 (1983) 470–475.
- [4] C. Nguyen, D.D. Do, A new method for the characterization of porous materials, *Langmuir* 15 (1999) 3608–3615.
- [5] P. Tarazona, U.M.B. Marconi, R. Evans, Phase equilibria of fluid interfaces and confined fluids-non-local versus local density functionals, *Mol. Phys.* 60 (1987) 573–595.
- [6] N.A. Seaton, J.P.R.B. Walton, N. Qljirke, A new analysis method for the determination of the pore size distribution of porous carbons from nitrogen adsorption measurements, *Carbon* 27 (1989) 853–861.
- [7] W.H. Press, S.A. Teukolsky, W.T. Vetterling, B.P. Flannery, *Numerical Recipes in FORTRAN: The Art of Scientific Computing*, Cambridge University Press, 1992.
- [8] P.H. Merz, Determination of adsorption energy distribution by regularization and characterization of certain adsorption isotherms, *J. Comput. Phys.* 38 (1980) 64–85.
- [9] W.A. House, M. Jaroniec, P. Brauer, P. Fink, Surface heterogeneity effects in nitrogen adsorption on chemically modified aerosols. II: adsorption energy distribution functions evaluated using numerical methods, *Thin Solid Films* 87 (1982) 323–335.
- [10] S.K. Bhatia, Determination of pore size distributions by regularization and finite element collocation, *Chem. Eng. Sci.* 53 (18) (1998) 3239–3249.
- [11] Z. Ryu, J. Zheng, M. Wang, B. Zhang, Characterization of pore size distributions on carbonaceous adsorbents by DFT, *Carbon* 37 (1999) 1257–1264.
- [12] F. Dion, A. Lasia, The use of regularization methods in the deconvolution of underlying distributions in electrochemical processes, *J. Electroanal. Chem.* 475 (1999) 28–37.
- [13] G.H. Golub, C.G. Van Loan, *Matrix Computations*, third ed., Johns Hopkins University Press, Baltimore, 1996.
- [14] H.D. Do, D.D. Do, A new diffusion and flow theory for activated carbon from low pressure to capillary condensation range, *Chem. Eng. J.* 84 (2001) 295–308.
- [15] A. Gil, S.A. Korili, G. Yu., Cherkashinin, extension of the Dubinin–Astakhov equation for evaluating the micropore size distribution of a modified carbon molecular sieve, *J. Colloid Interface Sci.* 262 (2003) 603–607.
- [16] C. Herdes, M.A. Santos, S. Abello, F. Medina, L.F. Vega, Search for a reliable methodology for PSD determination based on a combined molecular simulation –regularization–experimental approach, *Appl. Surf. Sci.* 252 (2005) 538–547.
- [17] L.A. Segura, P.G. Toledo, Pore-level modeling of isothermal drying of pore networks. Effects of gravity and pore shape and size distributions on saturation and transport parameters, *Chem. Eng. J.* 111 (2005) 237–252.
- [18] O. Solcova, L. Matejova, P. Schneider, Pore-size distributions from nitrogen adsorption revisited: models comparison with controlled-pore glasses, *Appl. Catal. A: Gen.* 313 (2006) 167–176.
- [19] P. Podkoscielny, K. Nieszporek, Heterogeneity of activated carbons in adsorption of phenols from aqueous solutions—comparison of experimental isotherm data and simulation predictions, *Appl. Surf. Sci.* 253 (2006) 3563–3570.
- [20] M. Jaroniec, T.J. Pinnavaia, M.F. Thorpe, *Access in Nanoporous Materials*, Plenum Press, New York, 1995.
- [21] K. Laszlo, P. Podkoscielny, A.D. Browski, Heterogeneity of polymer-based active carbons in adsorption of aqueous solutions of phenol and 2,3,4-trichlorophenol, *Langmuir* 19 (2003) 5287–5294.
- [22] K. Laszlo, E. Tombacz, P. Kerepesi, Surface chemistry of nanoporous carbon and the effect of pH on adsorption from aqueous phenol and 2,3,4-trichlorophenol solutions, *Colloids Surf. A: Physicochem. Eng. Aspects* 230 (2003) 13–22.
- [23] K. Laszlo, A. Szűcs, Surface characterization of polyethyleneterephthalate (PET) based activated carbon and the effect of pH on its adsorption capacity from aqueous phenol and 2,3,4-trichlorophenol solutions, *Carbon* 39 (2001) 1945–1953.
- [24] P.A. Gauden, A.P. Terzyk, M. Jaroniec, P. Kowalczyk, Bimodal pore size distributions for carbons: experimental results and computational studies, *J. Colloid Interface Sci.* 310 (2007) 205–216.
- [25] H.U. Kang, W. Kim, S.H. Kim, Pore size control through benzene vapor deposition on activated carbon, *Chem. Eng. J.* 144 (2008) 167–174.
- [26] J. Choma, J. Gorka, M. Jaroniec, Mesoporous carbons synthesized by soft-templating method: determination of pore size distribution from argon and nitrogen adsorption isotherms, *Microporous Mesoporous Mater.* 112 (2008) 573–579.
- [27] A. Shahsavand, M. Niknam Shahrak, Direct pore size distribution estimation of heterogeneous nano-structured solid adsorbents from condensation data: Condensation with no prior adsorption, *Colloids Surf. A: Physicochem. Chem. Eng. Aspects* 378 (2011) 1–13.
- [28] C. Nguyen, D.D. Do, Simple optimization approach for the characterization of pore size distribution, *Langmuir* 16 (2000) 1319–1322.
- [29] D.D. Do, *Adsorption Analysis: Equilibria Kinetics*, Imperial College Press, London, 1998.
- [30] P. Kowalczyk, A.P. Terzyk, P.A. Gauden, R. Leboda, E. Szmechtig-Gauden, G. Rychlicki, Z. Ryu, H. Rong, Estimation of the pore-size distribution function from the nitrogen adsorption isotherm. Comparison of density functional theory and the method of Do and co-workers, *Carbon* 41 (2003) 1113–1125.
- [31] T. Allen, *Particle Size Measurement*, 5th ed., Chapman & Hall, New York, USA, 1997.
- [32] G. Halsey, Physical adsorption on non-uniform surfaces, *J. Chem. Phys.* 16 (1948) 931–937.
- [33] G.C.P. Broekhoff, J.H. De Boer, Studies on pore systems in catalysis X. Calculation of pore distribution from the adsorption branch of nitrogen sorption isotherms in the case of open cylindrical pores. B. Applications, *J. Catal.* 9 (1967) 15–27.
- [34] M. Kruk, M. Jaroniec, J.M. Kim, R. Ryoo, Characterization of highly ordered MCM-41 silicas using X-ray diffraction and nitrogen adsorption, *Langmuir* 15 (1999) 5279–5284.
- [35] W. Stefaniak, J. Goworek, B. Bilinski, Pore size analysis by nitrogen adsorption and thermal desorption, *Colloids Surf. A: Physicochem. Eng. Aspects* 214 (2003) 231–237.
- [36] P.A. Gauden, A.P. Terzyk, P. Kowalczyk, Some remarks on the calculation of the pore size distribution function of activated carbons, *J. Colloid Interface Sci.* 300 (2006) 453–474.
- [37] P.I. Ravikovitch, A.V. Neimark, Characterization of nanoporous materials from adsorption and desorption isotherms, *Colloids Surf. A: Physicochem. Eng. Aspects* 187–188 (2001) 11–21.